Natural Convection in Shallow Cavities

Dae-Seok Bae*

Key Words : Shallow Cavity, Natural Convection, Finite-Volume Method, Secondary Cell, Correlation Equation.

Abstract

Natural convection heat transfer in a rectangular enclosure is investigated numerically for low aspect ratio(height/width) cavities. Numerical results are obtained for aspect ratios between 10^{-2} and 10^{0}, Rayleight numbers from 10^{3} to 10^{7} and Prandtl numbers from 10^{-2} to 10^{3}. Results are compared with existing analytical and experimental results. A heat transfer correlation is developed to predict the mean Nusselt number as a function of the three governing dimensionless parameters: Rayleigh number, aspect ratio and Prandtl number.

──────── Nomenclature ────────

A : aspect ratio(H/L)
g : gravitational acceleration
H : cavity height
h : heat transfer coefficient
k : thermal conductivity
L : cavity width
L1 : number of grids in the x-direction
M1 : number of grids in the y-direction
Nu : Nusselt number
P : pressure
p : dimensionless pressure

Pr : Prandtl number
T : temperature
T_c : cold wall temperature
T_h : hot wall temperature
U : horizontal velocity component
u : dimensionless horizontal velocity component
V : vertical velocity component
v : dimensionless vertical velocity component
X : horizontal coordinate
x : dimensionless horizontal coordinate
Y : vertical coordinate
y : dimensionless vertical coordinate

Greek
α : thermal diffusivity

* School of Mechanical & Automotive Engineering, Pukyong National University, Pusan, 608-026, Korea.

β : volumetric expansion coefficient

θ : dimensionless temperature

ν : kinematic viscosity

ρ : density

ψ : dimensionless stream function

1. Introduction

Natural convection in rectangular enclosures has been investigated for a long time in the literatures. Ostrach[1] has reviewed the large body of existing works and pointed out that such flows are affected greatly by the geometric configuration and the boundary conditions. May investigators in the past have studied natural convection in square or vertical rectangular cavities, but relatively little work has been done on natural convection in enclosures with low aspect ratios (ratio of height to width).

An asymptotic solution to this problem was presented by Cormack, Leal and Imberger[2], which is valid only in the limiting aspect ratio $H/L \to 0$ for fixed values of the Grashof and Prandtl numbers. Bejan and Tien[3] developed an asymptotic theory for small but finite aspect ratios and suggested a correlation for Nusselt number based on the three-regime theory(the $Ra \to 0$ regime, the intermediate regime and the boundary layer regime).

Experimental studies were performed by Imberger[4], Ostrach, Loka and Kumar[5], Sernas and Lee[6], and Kamotani, Wang and Ostrach[7]. Ostrach et al.[5] presented sketches of the secondary cell deformations in the end regions. Sernas et al.[6] visualized the secondary cell appearance in the shallow cavity using cigarette smoke. Kamotani et al.[7] pointed out the problems predicted by Bejan et al.[3] who assumed that the flow pattern has a simple unicell and that velocities are parallel

in the core region. Actually, the flow parttern is complex under certain conditions as surveyed in ref.[5~7]

There are also a few numerical studies available. Cormack, Leal and Seinfeld[8] obtained numerical solutions in the range of aspect ratio $0.05 \leq H/L \leq 1.0$ with $10 \leq Gr \leq 2 \times 10^4$ and $Pr=6.983$. Lee and Sernas[9] obtained solutions for an enclosure with an adiabatic as well as isothermal connecting walls for aspect ratios in the range $0.1 \leq H/L \leq 1.0$ with $10^6 \leq Gr(L/H)^3 \leq 3 \times 10^7$ and $Pr=0.7$. Shiralkar and Tien[10] obtained solutions in the range of aspect ratio $0.025 \leq H/L \leq 0.1$ with $10^3 \leq Ra \leq 6 \times 10^6 \leq$ and $10^{-2} \leq Pr \leq 10^2$, and proposed a modification to the correlation presented by Bejan and Tien[3] for $Pr \geq 1$, $H/L \geq 0.1$. They also suggested a correlation for low Prandtl numbers as a function of the Rayleigh number and the Prandtl number, but the correlation for the low Prandtl number is valid only in the boundary layer regime when Rayleigh number is high and the Nusselt number is independent of aspect ratio.

Present study aims to numerically investigate the effects of the Rayleigh number, aspect ratio, and Prandtl number on the flow and temperature fields to compare with existing analytical and experimental results, and to develop an improved correlation for the mean Nusselt number which covers a wide range of the Rayleight number, aspect ratio and the Prandtl number.

2. Mathmatical Formulation

The two-dimensional shallow enclosure is shown in Fig.1. The rectangular enclosure is bounded by two vertical walls at different temperatures, T_c and T_h, and two horizontal adiabatic walls.
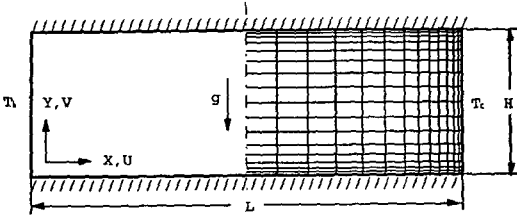
Fig.1 Enclosure geometry and grid system

Nondimensional governing equations for a steady and laminar natural convection flow of a Newtonian fluid with negligible viscous dissipation can be written as

Continuity;

$$\frac{\partial u}{\partial x} + \frac{\partial v}{\partial y} = 0 \tag{1}$$

X-momentum;

$$u\frac{\partial u}{\partial x} + v\frac{\partial u}{\partial y} = -\frac{\partial p}{\partial x} + \left(\frac{\partial^2 u}{\partial x^2} + \frac{\partial^2 u}{\partial y^2}\right) \tag{2}$$

Y-momentum;

$$u\frac{\partial v}{\partial x} + v\frac{\partial v}{\partial y} = -\frac{\partial p}{\partial y} + \left(\frac{\partial^2 v}{\partial x^2} + \frac{\partial^2 v}{\partial y^2}\right)$$

$$+ \frac{Ra}{Pr}\theta \tag{3}$$

Energy;

$$u\frac{\partial \theta}{\partial x} + v\frac{\partial \theta}{\partial y} = \frac{1}{Pr}\left(\frac{\partial^2 \theta}{\partial x^2} + \frac{\partial^2 \theta}{\partial y^2}\right) \tag{4}$$

where

$$x = \frac{X}{H}, \quad y = \frac{Y}{H}, \quad u = U\frac{H}{\nu}, \quad v = V\frac{H}{\nu},$$

$$p = \frac{PH^2}{\rho\nu^2}, \quad \theta = \frac{T - T_c}{T_h - T_c}, \quad Pr = \frac{\nu}{\alpha},$$

$$Ra = \frac{g\beta H^3(T_h - T_c)}{\alpha\nu} \tag{5}$$

The nondimensional boundary conditions are

$$u(0,y) = u(L/H,y) = u(x,0) = u(x,1) = 0$$

$$v(0,y) = v(L/H,y) = v(x,0) = v(x,1) = 0$$

$$\theta(0,y) = 1, \quad \theta(L/H,y) = 0$$

$$\partial\theta/\partial y = 0 \text{ at } y = 0 \text{ and } y = 1 \tag{6}$$

The local Nusselt number is defined as

$$Nu = \frac{hH}{k} = -\frac{\partial\theta}{\partial x}\bigg|_{wall} \tag{7}$$

and, the mean Nusselt number is calculated as

$$Nu = -\int_{wall}\left(\frac{\partial\theta}{\partial x}\right)_{x=0} dy \tag{8}$$

3. Numerical Procedure

The governing equations (1)~(4) were discretized using the finite-volume approach.[11] The SIMPLER algorithm was used to deal with linkage between the pressure and velocity. The staggered grid arrangement was used. The convection-diffusion terms in the momentum and energy equations were discretized by the power law scheme. The linearized equations were solved using a line-by-line TDMA(Tri Diagonal Matrix Algorithm), supplemented by a block-correction scheme.[12] The nonlinear coefficients are substituted successively with updated values. Under relaxation is required to ensure the convergence of the iterative procedure.

A non-uniform grid is used to generate a higher concentration near the wall boundaries in x- and y-directions. The grid spacing is generated by the following expressions:

$$XU(I) = \frac{L}{2H}\left[\frac{I-2}{L1/2-1}\right]^n \quad (I \le L1/2)$$

$$XU(I) = \frac{L}{2H} + \frac{L}{2H}\left[1 - \left(\frac{L1-I}{L1/2-1}\right)^n\right] \tag{9}$$
$$(I > L1/2)$$

$$YV(J) = \frac{1}{2}\left[\frac{J-2}{M1/2-1}\right]^n \quad (J \le M1/2)$$

$$YV(J) = \frac{1}{2} + \frac{1}{2}\left[1 - \left(\frac{M1-J}{M1/2-1}\right)^{n}\right]$$
$$(J > M1/2)$$

where XU(I) and YV(J) are the locations of control volume faces, L1 and M1 are the total number of grids in the x- and y-directions, respectively, and n determines the non-uniformity of the grid spacing. In order to ensure grid independence of the numerical solutions, several results were obtained for the case of Ra=10^6, Pr=7.0 and H/L=0.4 using various numbers of grids. As shown in Fig.2, the number of grid points in the x-direction (L1) varies from 28 to 66 with n=2, and the number in the y-direction(M1) varies from 18 to 42 with n=2. $\triangle X_{min}$ and $\triangle Y_{min}$ represent the minimum grid spacing next to the boundary walls. When $\triangle X_{min}$ or $\triangle Y_{min}$ is less than 0.005, the effect of grid spacing can be negligible. Thus, M1 is fixed($\triangle Y_{min}$=0.005) and L1 is varied so that $\triangle X_{min}$ is less than 0.005 as the aspect ratio changes. To keep a reasonable accuracy and to save computation time a grid system of 32×22 is used for aspect ratio H/L=0.4. With decreasing aspect ratio (H/L) the grid number in the x-direction is
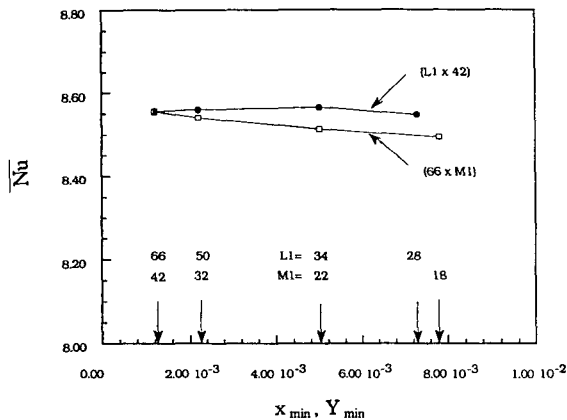
increased. A 202×22 grid system is used for H/L=0.01.

The iteration process was terminated when the following convergence criterion was satisfied at all internal grid points for all the variables B and the ratio of the mass residual in the computation domain to total flow rate was less than 10^{-7}.

$$\left|\frac{B_{i,j}^{m+1} - B_{i,j}^{m}}{B_{i,j}^{m}}\right| < 10^{-5} \tag{10}$$

Here B represents u, v or θ and m is the iteration order.

Preliminary solutions were obtained using a non-uniform grid of 22×22 for an aspect ratio H/L=1.0 and Pr=0.7, and were compared with the bench mark numerical solutions of de Vahl Davis[13] and of Hortmann et al.[14] As shown in Table 1 the agreement is very good within 1% error.

4. Results and Discussion

Sixty two solutions were obtained over the following range of conditions.

$$10^3 \le Ra \le 10^7$$
$$10^{-2} \le H/L \le 10^0$$
$$10^{-2} \le Pr \le 10^3$$

The ranges of the Rayleigh number and

Fig.2 Examination of grid dependence of numerical solutions at Ra=10^6, Pr=7.0 and H/L=0.4

Table 1 Comparison of the mean Nusselt number for a square cavity at Pr=0.7

Ra	10^3	10^4	10^5	10^6
$\overline{Nu}$[present]	1.122	2.254	4.528	8.747
$\overline{Nu}$[13]	1.118	2.243	4.519	8.800
$\overline{Nu}$[14]	–	2.245	4.522	8.825
$\varDelta\overline{Nu}/\overline{Nu}$[13]	0.367%	0.490%	0.199%	0.602%
$\varDelta\overline{Nu}/\overline{Nu}$[14]	–	0.401%	0.133%	0.884%

aspect ratio(H/L) sufficiently covered each of the three flow regimes proposed by Bejan and Tien.[3] The results in the Ra→0 regime and the intermediate regime are presented in Fig.3 and Fig.4, respectively, and the prediction by Bejan and Tien is also shown for comparison. The experimental date in the intermediate regime by Kamotani et al.[7] are plotted in Fig.4.

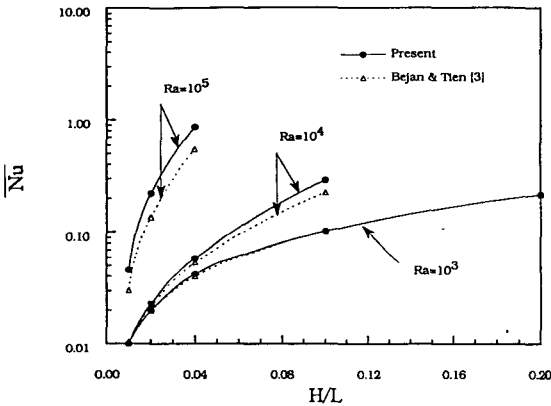The results in Fig.3 and Fig.4 should fall within the Ra→0 regime and the intermediate regime respectively.

Fig.3 Mean Nusselt number in the Ra→0 regime at Pr=7.0
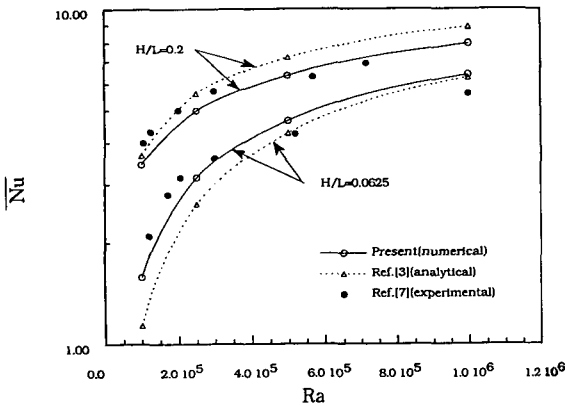

Fig.4 Mean Nusselt number in the intermediate regime at Pr=7.0

In the Ra→0 regime the agreement is very good at low Ra, but as the Ra and H/L increase the difference between the present numerical results and the prediction by Bejan and Tien increases. In the intermediate regime the agreement is somewhat worse than in the Ra→0 regime. In the analytical study Bejan and Tien assumed that the flow pattern in the shallow cavity is of a unicell in the intermediate regime, but previous experimental results[5~7] show that the flow pattern is very complex and depends on the Rayleigh number, aspect ratio and the Prandtl number. The experimental results given in Fig.4 are in good agreement with present numerical data.

The contour maps of streamlines and isotherms in an enclosure with adiabatic connecting walls are shown in Figs.5, 6 and 7. The stream function field is divided basically into six intervals in the range of $0 \leq |\psi| \leq |\psi|_{max}$. If two $|\psi|_{max}$ exist in the cavity and secondary cells appear, two inner streamlines are added to show the secondary cells.

The effect of the Rayleigh number on the flow pattern is shown in Fig.5. When the Rayleigh number is 10^3, the streamline pattern shows the typical two major regimes: a core region which contains nearly parallel flow with
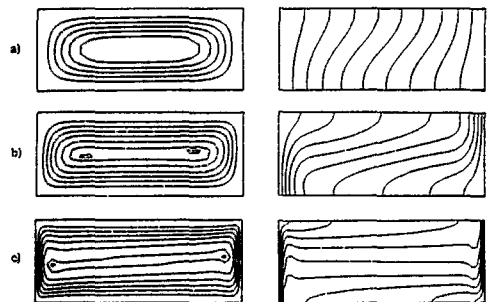

Fig.5 Contour maps of streamlines and isotherms for the various Ra at H/L=0.4 and Pr=7.0 (a) Ra=10^3 b) Ra=10^4 c) Ra=10^6)

warmer fluid in the upper half of the cross-section, and end regions where the flow is turned around 180 degrees. As the Rayleigh number increases, secondary cells appear in the end regions, and the flow pattern in the core region is no longer parallel. At a large Rayleigh number(Ra=10^6) the temperature gra-dients are more steeper near the vertical walls, and the temperature in the core becomes stra-tified.

The effect of aspect ratio(H/L) is shown in Fig.6. Secondary cells appear in all cases. With decreasing H/L a third cell which looks like an inner cell of the unicell appears in the middle of the cavity, and the flow pattern in the core region becomes more parallel. As the aspect ratio H/L decreases, the thermal boun-dary layer on the vertical wall is gradually destroyed and convective effects are not sig-nificant near the end walls. From this con-sideration it can be said that the secondary cells in the very low aspect ratio cavity(H/L ≪1) are weak and do not effect significantly on heat transfer which merely act as a center of rotation.

The effect of Prandtl number is shown in Fig.7. As the Prandtl number decreases the flow pattern becomes a unicell but with in-
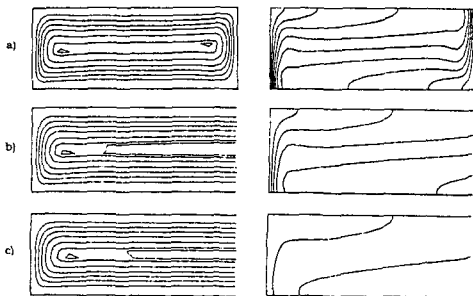
clination. The appearnace of secondary cells was theoretically predicted by Cormark et al.[2], and Cormack et al.[8] observed the value of $Ra^2(H/L)^3$ at which the core flow changes from parallel to nonparallel. They estimated that the appropriate limit for validity of the parallel flow structure is $2.5 \times 10^5 \leq Ra^2(H/L)^3 \leq 2 \times 10^6$. The asymptotic theory on which that is based
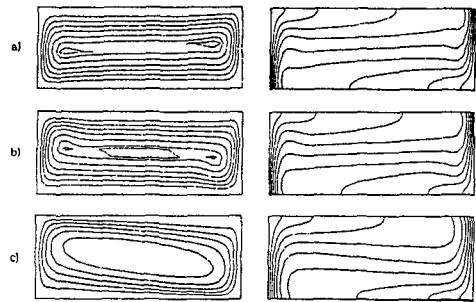
Fig.7 Contour maps of streamlines and isotherms for the various Pr at Ra=10^5 and H/L=0.4 (a) Pr=1,000 b) Pr=1.0 c) Pr=0.1)

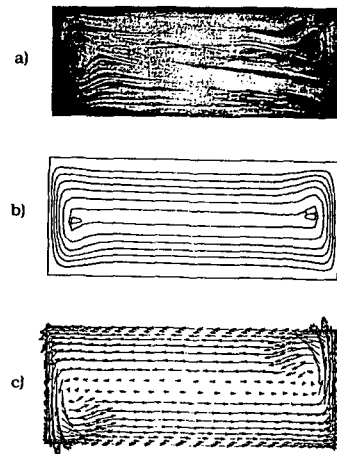**Fig.8** Comparison between experimental results of Sernas & Lee[6] and the present numerical results at Ra=2.44×10^5, Pr=0.7 and H/L=0.4 (a) experimental smoke pattern b) numerical streamlines c) numerical velocity vectors)

Fig.6 Contour maps of streamlines and isotherms for the various H/L at Ra=10^5 and Pr=7.0 (a) H/L=0.4 b) H/L=0.1 c) H/L=0.04)

is valid when $H/L \leq 0.1$ and $Ra^2(H/L)^3 \leq 10^5$. Present numerical results confirm this, but the non-parallel flow in the core region does not always predict the secondary cell appearance. As shown in Fig.7(c) the flow pattern in core region is non-parallel without secondary cells near the end walls, and as shown in Fig.6(c) the flow pattern in the core region is almost parallel with secondary cells near the end walls. From the above observations we know that the appearance of secondary cell is a complex function of the Rayleigh number and aspect ratio as well as the Prandtl number.

The smoke patterns from the experimental study by Sernas and Lee[6], and streamlines and velocity vectors from the present numerical study are presented in Fig.8. In this figure the numerical boundary conditions are the same as those of the experiment for comparison. The left wall is cold, the right wall is hot and the horizontal walls are taken as isothermal. The experimental smoke pattern is similar to the numerical streamlines. The velocity vectors show the deformation of the secondary cells in the end region and agree well with sketch of the dye-line deformation near the hot wall presented by Ostrach et al.[5].

The results in the boundary layer regime are shown in Fig.9. The agreement between the numerical results and the prediction is good at the high Rayleigh number($Ra=10^7$). When the Rayleigh number is 10^6 the agreement is not so good and the difference is increased with increasing aspect ratio(H/L). In our notation the following correlation by Bejan and Tien[3] is used,

$$Nu = A \cdot \left(1 + \left\{ \left[\frac{(Ra \cdot A)^2}{362,880} \right]^n + \left[0.623 \frac{Ra^{1/5}}{A} \right]^n \right\}^{1/n} \right) \qquad (11)$$
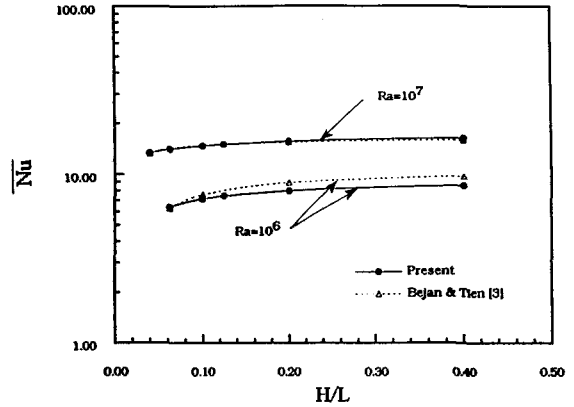

Fig.9 Mean Nusselt number in the boundary layer regime at Pr=7.0

where $n = -0.386$. Here, the boundary layer regime Nusselt number was predicted to be

$$Nu = 0.623 \cdot \gamma \cdot Ra^{1/5} \qquad (12)$$

In this equation γ has been replaced by unity for simplicity. This indicated that the heat transfer is independent of aspect ratio(H/L) in the boundary layer regime. However there is some effect of aspect ratio as shown in Fig.9 so that it is more appropriate to replace γ by $\gamma = \gamma(A)$. Shiralkar and Tien[10] considered the effect of aspect ratio(H/L) on heat transfer in the boundary layer regime. They proposed the following modification to equation (11) for $Pr \geq 1$, $A \leq 0.1$.

$$Nu = A \cdot \left(1 + \left\{ \left[(Ra \cdot A)^2 \frac{\gamma_1(A)}{362,880} \right]^n + [\gamma_2(A) \cdot Ra^{0.2}/A]^n \right\}^{1/n} \right) \qquad (13)$$

Where $n = -0.386$ and

$$\gamma_1(A) = (0.811 - 6.433 \times 10^{-3}/A)^{-2.5907}$$
$$\gamma_2(A) = (1.2425 + 4.5 \times 10^{-4}/A)^{-2.5907} \qquad (14)$$

The results of the present study are compared in Table 2 with equation (13). It is seen that this correlation is appropriate at high

Prandtl numbers and the effect of the Prandtl number on heat transfer is substantial for Pr ≤ 1.0. They also proposed the following correlation for Pr<1.

$$Nu = 0.35 \cdot Ra^{1/4} \mathrm{Pr}^{1/4} \qquad (15)$$

This expression is expected to be applied for laminar flow in shallow and square enclosures and is obtained for the asymptotic condition, Ra$\to\infty$. However, it is not appropriate to apply this equation in the shallow cavity for general use because the Nusselt number is affected by the aspect ratio(H/L) at low Prandtl numbers as shown in Fig.10.

It would be useful to develop a general correlation of the mean Nusselt number including Rayleigh number, aspect ratio(H/L) and Prandtl number effects for a shallow cavity with adiabatic horizontal walls. Based on the present numerical results and a heat transfer relationship presented by Berkovsky and Polevikov(as cited in ref[15]) the following modification to equation (13) is proposed.
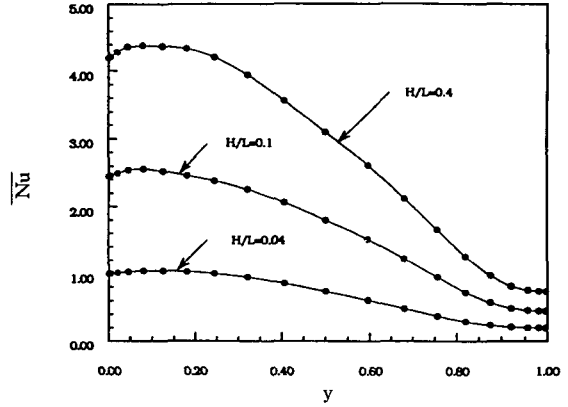

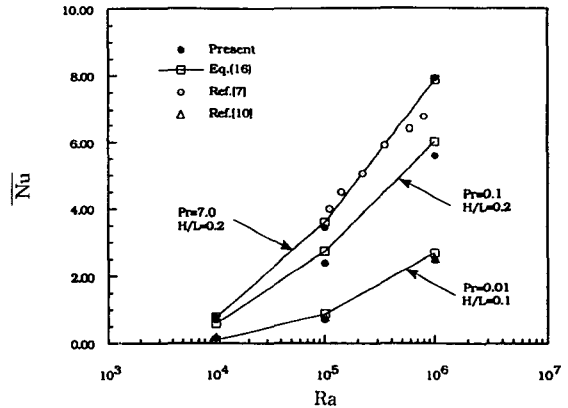**Fig.10** Local Nusselt number for various H/L at Ra=10^5 and Pr=0.1

Fig.11 Comparison between the present correlation of mean Nusselt number Eq[16] and various numerical and experimental results

$$Nu = 0.95 \cdot A \cdot \left(\frac{\mathrm{Pr}}{\mathrm{Pr}+0.2} \right)^{0.37}$$
$$\left(1 + \left\{ \left[(Ra \cdot A)^2 \frac{\gamma_1(A)}{362,880} \right]^n \right. \right.$$
$$\left. \left. + [\gamma_2(A) \cdot Ra^{0.2}/A]^n \right\}^{1/n} \right) \qquad (16)$$

Here n= -0.386 and $\gamma_1(A)$, $\gamma_2(A)$ are the same as eq.(14). This expression covers a wide range of conditions: 10^{-2}<Pr<10^3, 10^3< Ra<10^7 and 10^{-2}<H/L<10^0. The mean deviation from the numerical results is 4.3 percent.

Table 2 The effect of Prandtl number on the mean Nusselt number and comparison of the present numerical results and the correlation by Shiralkar and Tien[10] at H/L=0.2

Ra=	10^4	10^5	10^6
Eq [13]	0.8437	3.8169	8.3545
Pr=1,000.0	0.8229	3.4545	7.9564
100.0	0.8229	3.4543	7.9565
7.0	0.8277	3.4475	7.9435
1.0	0.8180	3.3086	7.5620
0.7	0.8137	3.2275	7.3557
0.1	0.7010	2.3939	5.5920
0.01	0.3600	1.1507	3.3035

Results from Eq.(16) are plotted and com-
pared with existing experimental and numeri-
cal results in Fig.11. The agreement is so
good that this correlation could be used to
predict the Nusselt number in shallow cavi-
ties with adiabatic horizontal walls usefully
over a wide range of conditions.

5. Conclusion

A numerical study has been carried out for
the problem of natural convection heat tran-
sfer in a horizontal shallow cavity containing
two opposed vertical isothermal surfaces at
different temperature and two horizontal adia-
batic connecting walls.

The present numerical results are in good
agreement with the existing experimental re-
sults and show appearance of the secondary
cells. The existence of the secondary cells is
a complex function of the Rayleigh number,
aspect ratio(H/L) and the Prandtl number. As
the Rayleigh number and Prandtl number are
increased, the secondary cells appear near the
end walls, and as the aspect ratio is decre-
ased the secondary cells appear near the end
walls, and as the aspect ratio is decreased the
secondary cells are weak and the third cell
which looks like an inner cell of the unicell
appears in the core region.

A correlation equation for the mean Nu-
sslet number has been developed, which is
valid for natural convection over a wide range
of the Rayleigh number, aspect ratio and the
Prandtl number in shallow cavities.

References

(1) Ostrach, S., "Natural convection in en-
closures", Advances in Heat Transfer,
Vol. 8, 1972, pp. 161~227.

(2) Cormark, D.E., Leal, L.G., and Imberger,
J., 1974, "Natural convection in a shallow
cavity with differentially heated end walls.
Part 1. asymptotic theory", Journal of
Fluid Mechanics, Vol. 65, pp. 209~229.

(3) Bejan, A. and Tien, C.L., 1978, "Laminar
natural convection heat transfer in a ho-
rizontal cavity with different end tempe-
ratures", Journal of Heat Transfer, Vol.
100, No. 4, pp. 641~547.

(4) Imberger, J., 1974, "Natural convection in
a shallow cavity with differentially heated
end Walls. Part 3. experimental results",
Journal of Fluid Mechanics, Vol. 65, pp.
247~260.

(5) Ostrach, S., Loka, R.R., and Kumar, A.,
1980, "Natural convection in low aspect
ratio rectangular enclosures", Natural Con-
vection in Enclosures, ASME HTD-Vol.
8, pp. 1~10.

(6) Sernas, V. and Lee, E.I., 1987, "Heat
transfer in air enclosures of aspect ratio
less than one", Journal of Heat Transfer,
Vol. 103, pp. 617~622.

(7) Kamotani, Y., Wang, L.W., and Ostrach,
S., 1983, "Experiments on natural con-
vection heat transfer in low aspect ratio
enclosures", AIAA Journal, pp. 290~294.

(8) Cormack, D.E., Leal, L.G., and Seinfeld,
J.H., 1974, "Natural convection in a sha-
llow cavity with differentially heated end
walls. Part 2. numerical solutions", Jour-
nal of Fluid Mechanics, Vol. 65, pp. 231
~246.

(9) Lee, E.I. and Sernas, V., 1980, "Numerical
study of heat transfer in rectangular air
enclusures of aspect ratio less than one",
ASME paper 80-WA/HT--43.

(10) Shiralkar, G.S. and Tien, C.L., 1981, "A
numerical study of laminar natural con-
vection in shallow cavities", Journal of

Heat Transfer, Vol. 103, pp. 226~231.

(11) Patankar, S.V., 1980, "Numerical heat tran-sfer and fluid flow", Hemisphere Pub. Co.

(12) Patankar, S.V., 1981, "A calculation pre-cedure for two-dimensional Elliptic situ-ations", Numerical Heat Transfer, Vol. 4, pp. 409~425.

(13) de Vahl Davis, G., 1983, "Natural convec-tion of air in a square cavity: A bench mark numerical solution", Int. J. for Nu-merical Methods in Fluids, Vol. 3, pp. 249~264.

(14) Hortmann, M., Peric, M., and Scheuerer, G., 1990, "Finite volume multigrid predic-tion of laminar natural convection: Bench mark solutions", Int. J. for Numerical Methods in Fluids, Vol. 11, pp. 189~207.

(15) Gebhar, B., Jaluria, Y., Mahajan, R.L., and Sammakia, B., 1988, Buoyancy Induced Flows and Transport, Hemisphere Pub. Co.